

known, more attention should be focused on the rotational and translational energy distributions in attempting to reconcile the detailed balancing calculations.

The present study and other reports^{9,12-14} have shown that simultaneous chemiluminescence observations from multiple vibrational states can lead to errors in the measurements of rate constants and product yields. Some of these errors, while quite subtle, can be large. These results argue strongly for the ap-

plication of selected single state observations and analyses in IRCL measurements.

Acknowledgment. We gratefully acknowledge the Department of Energy for support of this research program and the National Science Foundation for the laser equipment. D.A.D. thanks the National Bureau of Standards for support through a National Research Council postdoctoral fellowship.

Photocatalytic Activity of TiO₂ Powders Suspended in Aqueous Silver Nitrate Solution. Correlation with pH-Dependent Surface Structures

Bunsho Ohtani,* Yoshitaka Okugawa, Sei-ichi Nishimoto, and Tsutomu Kagiya

Department of Hydrocarbon Chemistry, Faculty of Engineering, Kyoto University, Sakyo-ku, Kyoto 606, Japan
(Received: July 18, 1986)

Photocatalytic ($\lambda_{\text{ex}} > 300$ nm) activity of anatase and rutile TiO₂ powders suspended in AgNO₃ solution was investigated at room temperature under Ar. The initial rate of the photocatalytic reaction producing O₂ and Ag metal strongly depended upon the pH of suspension, i.e., it decreased with decreasing pH, becoming negligible at pH < 2 with anatase and pH < 5 with rutile, respectively. The amount of Ag⁺ adsorbed on the TiO₂ surfaces in the dark decreased with decreasing pH from 8 to 2. The pH dependence of TiO₂ activity was attributed predominantly to the Ag⁺ adsorption; the initial rates of the photocatalytic reactions by both anatase and rutile TiO₂ were in proportion to the amount of surface-adsorbed Ag⁺. The characterization of surface hydroxyl groups on the TiO₂ powders by means of potentiometric titration of the aqueous suspensions revealed that decreasing the pH causes the protonation of neutral hydroxyl groups into positively charged ones, which inhibits the Ag⁺ adsorption.

Introduction

A common feature of the photocatalytic reaction by suspended semiconductor powders in aqueous solutions¹ is the remarkable pH dependence of the reaction rate. Such pH-dependent photocatalytic activities of TiO₂/Pt have been demonstrated for dehydrogenation of alcohols,² decomposition of carboxylic acids,³ carbohydrate,⁴ and hydroxylamine,⁵ molecular weight increase or decrease of poly(ethylene oxide),⁶ oxidation of aromatic compounds,⁷ and N-alkylation of amines.⁸ Although the characterization of the pH-dependent photocatalytic action of semiconductor suspensions seems to be quite important, there are few satisfactory studies because of the complexity of photocatalytic systems.

We have previously demonstrated photocatalytic O₂ evolution and Ag metal deposition by metal-unloaded TiO₂ suspended in aqueous silver salt solutions.⁹ In the present work, the pH de-

pendence of reaction rate in this simple photocatalytic system was studied with simultaneous characterization of the amount of adsorbed Ag⁺ and hydroxyl groups on the TiO₂ surface. The role of the surface-adsorbed Ag⁺ as an electron scavenger in the enhancement of water oxidation is discussed.

Experimental Section

Anatase and rutile TiO₂ powders were supplied from Merck and Wako Pure Chemicals (Osaka, Japan, practical grade), respectively, and used without further activation. The specific surface area of these powders was evaluated from nitrogen adsorption at -196 °C based on the BET equation. The other materials were used as received. Water was passed through ion-exchange resin and distilled before use; the purity was checked by the conductivity of <0.2 $\mu\text{S cm}^{-1}$.

The finely ground TiO₂ powder (250 mg) was suspended in 2.00 $\times 10^{-3}$ -1.00 $\times 10^{-2}$ mol dm⁻³ AgNO₃ aqueous solution (5.0 cm³, containing 9 $\times 10^{-2}$ mol dm⁻³ KNO₃) in a glass tube (18 mm in diameter and 180 mm in length, transparent for the light of wavelength >300 nm). The pH of the suspension was adjusted by adding 1.00 $\times 10^{-1}$ mol dm⁻³ NaOH or HNO₃ (<0.15 cm³). The suspension was sonicated for 5 min, purged with Ar for >30 min, and then sealed off with a rubber stopper. Irradiation was performed with a 400-W high-pressure mercury arc at 27 \pm 2 °C. The TiO₂ suspension was magnetically stirred throughout the irradiation. Product analyses were performed as described elsewhere.⁹ Quantum efficiency was conveniently estimated by using a Blak-Ray J-221 ultraviolet meter on the assumption that the incident light consists of photons at 365 nm.

The amount of Ag⁺ adsorbed on the TiO₂ surface in the dark, under conditions similar to the photocatalytic reaction, was de-

(1) For a review see: Bard, A. J. *J. Phys. Chem.* **1982**, *86*, 172.
(2) (a) Kawai, T.; Sakata, T. *Chem. Lett.* **1981**, 81. (b) Nishimoto, S.; Ohtani, B.; Sakamoto, A.; Kagiya, T. *Nippon Kagaku Kaishi* **1984**, 246. (c) Nishimoto, S.; Ohtani, B.; Shirai, H.; Kagiya, T. *J. Polym. Sci., Polym. Lett. Ed.* **1985**, *23*, 141. (d) Nishimoto, S.; Ohtani, B.; Kagiya, T. *J. Chem. Soc., Faraday Trans. 1* **1985**, *81*, 2467. (e) Nishimoto, S.; Ohtani, B.; Shirai, H.; Kagiya, T. *J. Chem. Soc., Perkin Trans. 2* **1986**, 661.
(3) (a) Kraeutler, B.; Bard, A. J. *J. Am. Chem. Soc.* **1978**, *100*, 5985. (b) Yoneyama, H.; Takao, Y.; Tamura, H.; Bard, A. J. *J. Phys. Chem.* **1983**, *87*, 1417. (c) Sakata, T.; Kawai, T.; Hashimoto, K. *J. Phys. Chem.* **1984**, *88*, 2344.
(4) St. John, M. R.; Furgala, A. J.; Sammells, A. F. *J. Phys. Chem.* **1983**, *87*, 801.
(5) Oosawa, Y. *J. Phys. Chem.* **1984**, *88*, 3069.
(6) Nishimoto, S.; Ohtani, B.; Shirai, H.; Adzuma, S.; Kagiya, T. *Polym. Commun.* **1985**, *26*, 292.
(7) Fujihira, M.; Satoh, Y.; Osa, T. *Bull. Chem. Soc. Jpn.* **1982**, *55*, 666.
(8) Nishimoto, S.; Ohtani, B.; Yoshikawa, T.; Kagiya, T. *J. Am. Chem. Soc.* **1983**, *105*, 7180.

(9) Nishimoto, S.; Ohtani, B.; Kajiwar, H.; Kagiya, T. *J. Chem. Soc., Faraday Trans. 1* **1983**, *79*, 2685.

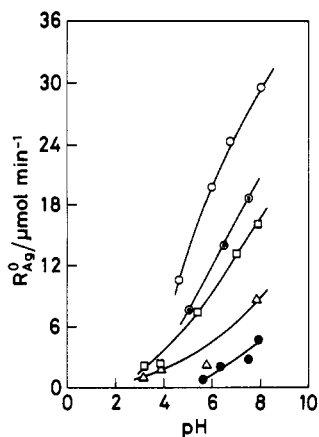


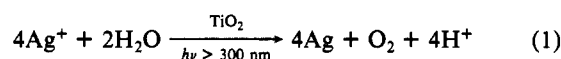
Figure 1. pH dependence of initial rate of photocatalytic Ag metal deposition (R_{Ag}^0) from AgNO₃ solution (5.00 cm³). Initial concentrations of AgNO₃ are as follows: ○, 1.00×10^{-2} ; □, 5.00×10^{-3} ; △, 3.00×10^{-3} ; ●, 2.00×10^{-3} mol dm⁻³ with anatase TiO₂ (250 mg); and ●, 3.00×10^{-3} mol dm⁻³ with rutile TiO₂ (250 mg).

terminated from the difference between the Ag⁺ concentrations before and after addition of TiO₂ at various pH's and concentrations of AgNO₃. The measurement was carried out in a 200-cm³ flat-bottom Pyrex jar equipped with glass and double-junction type reference electrodes (Horiba 1026A-06T and 2530A-06T, respectively), thermometer, inlet and outlet for purified N₂ gas, and microburet.^{10,11} The outer and inner chambers of the reference electrode were filled with KNO₃ and KCl aqueous solutions, respectively, to avoid precipitation of AgCl. The cell was kept at a constant temperature (27.0 ± 0.2 °C) by circulating thermostated water through an outer jacket around the cell. An Ag⁺ selective electrode (Horiba 8011-06T) was used with a Hitachi-Horiba M-8s pH-mV meter calibrated with standard AgNO₃ solutions (10^{-2} – 10^{-5} mol dm⁻³ AgNO₃ in 9×10^{-2} mol dm⁻³ KNO₃). The TiO₂ powder (anatase or rutile, 5.00 g) was added to the AgNO₃ solution (100 cm³, 2.00×10^{-3} – 1.00×10^{-2} mol dm⁻³ in 9×10^{-2} mol dm⁻³ KNO₃) in the cell. Thus, the Ag⁺ adsorption measurement was carried out on a 20-times larger scale than the photocatalytic reaction, for convenience. A small portion (0.05–0.15 cm³) of NaOH or HNO₃ (1.00×10^{-1} mol dm⁻³) was added to the magnetically stirred suspension of TiO₂ for the pH adjustment. Stirring for ca. 30 min was required to obtain the equilibrium value of pH of the suspension.

The amount of surface hydroxyl groups was evaluated by titration of a TiO₂ suspension in 100 cm³ of 7×10^{-4} mol dm⁻³ KOH with 1.00×10^{-2} mol dm⁻³ HNO₃ in an N₂ atmosphere with magnetic stirring. The titration was operated in the Pyrex cell as used for the Ag⁺ adsorption measurement. Particular attention was paid to exclusion of CO₂ from the solution and titrant.

Results and Discussion

Photocatalytic Reaction of TiO₂-Suspended Aqueous AgNO₃ Solution. Photoirradiation ($\lambda_{ex} > 300$ nm) of TiO₂ suspended in an aqueous AgNO₃ solution led to the liberation of O₂ in the gas phase of the reaction mixture and concomitant deposition of silver metal on the TiO₂ surface, as reported previously.⁹ The stoichiometry is as follows.



According to eq 1, the pH of the reaction mixture decreased as the photocatalytic reaction proceeded. This pH decrease is undesirable for the evaluation of the pH-dependent rate of the photocatalytic reaction. In fact, the rate decreased drastically over the photoirradiation period up to 8 h and was recovered by the addition of NaOH,⁹ showing that the pH decrease due to reaction 1, and not the inner-filter effect of deposited Ag, is

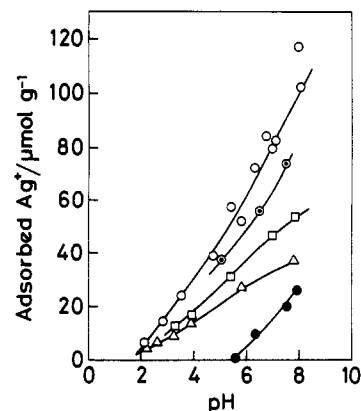


Figure 2. pH dependence of the Ag⁺ adsorption on TiO₂ surfaces. Symbols are the same as in Figure 1.

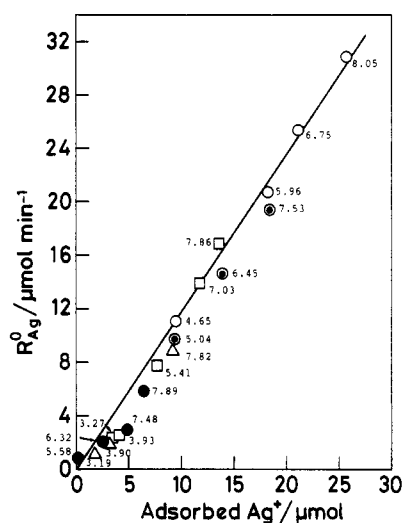


Figure 3. Correlation between the initial rate of photocatalytic Ag metal deposition (R_{Ag}^0) and the amount of Ag⁺ adsorbed on TiO₂. Symbols are the same as in Figures 1 and 2. Number denotes pH of the suspension.

responsible for the decreased rate. Therefore, in the present work the rate was measured within a short period of the irradiation, e.g., 10–30 s to avoid appreciable pH change, under the conditions of various concentrations of AgNO₃ and pH's of the suspension. The initial rate of the Ag metal deposition (R_{Ag}^0) is shown in Figure 1. A blank experiment revealed the negligible formation of silver nuclei (< 0.1 μmol min⁻¹) in the absence of TiO₂ under the present photoirradiation conditions.

In the case of anatase TiO₂, almost no deposition of Ag metal could be detected in the pH region of < 2 . Dissolution of the deposited silver metal at such lowered pH was not observed. The initial rate increased significantly with pH increase from 2 to 8, at each concentration of Ag⁺ (2.00×10^{-3} – 1.00×10^{-2} mol dm⁻³). At a given pH of suspension the rate increased with increasing Ag⁺ concentration. Similarly, photocatalytic activity of rutile TiO₂ was negligible at pH < 5 and increased with the pH increase (5–8), though rutile TiO₂ led to a relatively small R_{Ag}^0 compared with anatase TiO₂ in a 3.00×10^{-3} mol dm⁻³ AgNO₃ solution. Further increases of pH (> 8) formed a brown precipitate of Ag₂O and drastically lowered the Ag⁺ concentration in both suspensions. Under these conditions, since the pH would decrease as the photocatalytic reaction proceeds, the rate was reduced to be nearly zero. This is consistent with the fact that the time-course curve became a plateau by the prolonged irradiation of a nonbuffered aqueous suspension of anatase TiO₂ and the fact that the photocatalytic reaction proceeded monotonously in a buffered solution of AgF.⁹

On the other hand, a quite similar pH dependence was observed for the Ag⁺ adsorption onto the TiO₂ surface in the dark (Figure 2). The amount of Ag⁺ adsorbed ($[Ag^+]_{ads}$) on the anatase TiO₂

(10) Parks, G. A.; de Bruyn, P. L. *J. Phys. Chem.* **1962**, *66*, 967.

(11) Butler, M. A.; Ginley, D. S. *J. Electrochem. Soc.* **1978**, *125*, 231.

TABLE I: Properties of Hydroxyl Groups on the Surface of Anatase and Rutile TiO₂ Powders Evaluated by Potentiometric Titration of the Suspensions

TiO ₂	A, ^a m ² g ⁻¹	S, ^b μmol g ⁻¹	pK _{a1}		pK _{a2}		pH _{EABP} ^c	pH _{ip} ^d
			a	b	c	d		
anatase	10	21.4	6.29	-52.0	7.49	58.9	6.89	6.89
rutile	13	133	5.76	-12.2	8.38	20.8	7.07	7.00
P-25 ^e	56	460	4.98	-26.4	7.80	13.1	6.39	6.4

^a Specific surface area measured with BET equation. ^b Total amount of surface hydroxyls obtained by extrapolation of plots for 1/Γ⁺ (or 1/Γ⁻) vs. 1/C_H (or 1/C_{OH}). ^c pH of equi-acid-base point; (a + c)/2 (see text). ^d pH of the intersection of the titration curves (Figure 1). ^e Reported values for anatase-rutile mixed TiO₂ (supplied by Degassa, see ref 18).

decreased with decreasing pH, becoming negligible at pH < 2. The Ag⁺ adsorption on rutile TiO₂ was negligible at pH < ca. 5 and increased with the pH increase at pH > 6. In the pH region studied (2–6), [Ag⁺]_{ads} on the anatase surface was larger than that on the rutile surface.

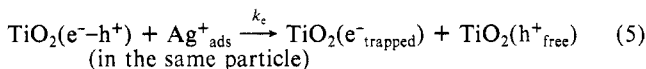
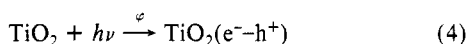
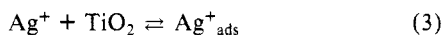
Comparison of data shown in Figures 1 and 2 led to a simple correlation that the rate of the photocatalytic reaction is proportional to [Ag⁺]_{ads} with both anatase and rutile TiO₂ (Figure 3). Thus, the rate is formally represented as follows.

$$R_{\text{Ag}}^0 / \mu\text{mol min}^{-1} = 1.18 [\text{Ag}^+]_{\text{ads}} / \mu\text{mol} \quad (2)$$

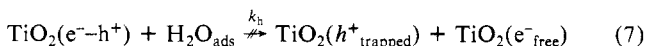
This agrees with the previous work by Fleischauer and co-workers on the photoreaction by single-crystal TiO₂ immersed in an aqueous AgNO₃ solution.¹²

Noticeable is the fact that the same [Ag⁺]_{ads} (this can be achieved at the appropriate condition of concentrations of AgNO₃ and pH's) gives practically the same R_{Ag}⁰ value despite the significantly different pH values (e.g., >3 units of pH varied at [Ag⁺]_{ads} ≈ 9 μmol on 250 mg of the anatase TiO₂; see Figure 3). Consequently, pH-dependent factors other than the Ag⁺ adsorption, such as protonation-deprotonation equilibria of surface hydroxyl groups or aggregation of TiO₂ particles,¹³ have negligible direct but possibly indirect influences on the photocatalytic activity under these conditions. The indirect influence of the equilibria of surface hydroxyl groups is discussed in the last section.

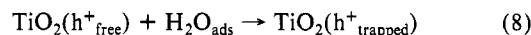
Mechanism of TiO₂ Photocatalysis in AgNO₃ Solution. The photophysical processes involved in an irradiated TiO₂ particle which adsorbs Ag⁺ are given in eq 3–6. This scheme assumes



that irradiation of the TiO₂ gives no significant effect on the adsorption isotherm established in the dark. The surface-adsorbed Ag atom is most likely as the chemical expression of TiO₂(e^{-trapped}) in reaction 5. Recently, Ward and Bard have illustrated an essentially identical scheme for the photocatalytic redox reaction involving acetate and high-valent transition-metal ions,¹⁴ although the adsorption behavior of the solution species has not been described explicitly. Furthermore, they considered the oxidation of acetate with a hole as more rapid than the reduction of metal ion with an electron. In the present system containing no hole scavengers, however, the experimental results indicate that the electron trappings can proceed predominantly and diminish the extent of unfavorable recombination of the electron-hole pair (TiO₂(e^{-trapped})). Hole trappings by surface-adsorbed H₂O and/or surface hydroxyls are negligible.



Free charge, TiO₂(h⁺_{free}), produced by way of the trapping reactions must be long-lived relative to TiO₂(e^{-trapped}) because of the absence of geminate recombination, and it will eventually oxidize the surface species.

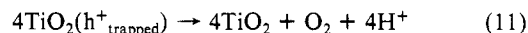
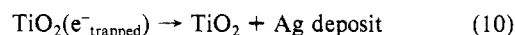


Under a photostationary state, the faster relaxation processes of TiO₂(e^{-trapped}) should determine the quantum yield for the charge separation resulting in trapped holes and electrons, which is given in the form

$$\Phi(h^+_{\text{trapped}}) = \Phi(e^-_{\text{trapped}}) = \varphi(e^-h^+) \frac{k_e N_e + k_h N_h}{k_e N_e + k_h N_h + 1/\tau_0} \quad (9)$$

where N_e and N_h represent numbers of surface adsorbates for individual charge trappings, φ(e^{-trapped}) is the efficiency of the excitation of an electron from the valence band into the conduction band, and τ₀ is the intrinsic lifetime of TiO₂(e^{-trapped}). An approximately linear relation between Φ(e^{-trapped}) and N_e (amount of Ag⁺ adsorbed on the surface) is derived under the conditions where k_h is negligible and 1/τ₀ is relatively large compared to k_eN_e. This is consistent with the fact that the largest R_{Ag}⁰ (evaluated from eq 2 and 22 as 27 μmol min⁻¹ at pH 7) corresponded to the quantum efficiency of ca. 0.5 estimated roughly from the incident photon flux.

A further assumption for the subsequent chemical reactions at the TiO₂ surface is that the trapped electrons and holes can irreversibly produce the observed products without undergoing surface recombination. The net reactions are represented as eq 10 and 11. Although we have at present no structural evidence,



formation of intermediate species such as hydroxyl radicals and hydrogen peroxides is plausible in the course of the trapped-hole reactions (eq 11). In contrast to the rather complicated behavior of hole reactions, reaction of an electron trapped by adsorbed Ag⁺ to produce Ag deposit can be readily realized in light of the redox potential for the Ag⁺/Ag couple (+0.56 V vs. SCE) that is positive of the potential of photoelectrons in the TiO₂.¹⁵

Characterization of Hydroxyl Groups on the TiO₂ Surface. The amphoteric nature of aqueous suspension of metal oxides, such as TiO₂, has been documented to be attributable to chemisorbed water, i.e., hydroxyl groups on their surface.¹⁶ Measurement of the surface hydroxyls has been carried out by means of acid-base titration,^{10,11} substitution with fluoride anion,¹⁶ or esterification with organic acids.¹⁷ In this work, hydroxyl groups on the surface of TiO₂ powders were quantitatively characterized by the titration method.

Figure 4 shows the titration curves for the anatase and rutile TiO₂ powders suspended in aqueous KOH solution. A titration curve for the aqueous KOH solution without TiO₂ is also plotted. As is clearly seen, the pH values decreased in the alkaline region and increased in the acidic region by the addition of either the anatase or the rutile TiO₂ powder. In each system the titration

(12) Fleischauer, P. D.; Alan Kan, H. K.; Shepherd, J. R. *J. Am. Chem. Soc.* **1972**, *94*, 283.

(13) Curran, J. S.; Domenech, J.; Jaffrezic-Renault, N.; Philippe, R. *J. Phys. Chem.* **1985**, *89*, 957.

(14) Ward, M. D.; Bard, A. J. *J. Phys. Chem.* **1982**, *86*, 3599.

(15) Dobos, D. *Electrochemical Data*; Elsevier: Amsterdam, 1975; p 149.

(16) Boehm, H. P. *Discuss. Faraday Soc.* **1971**, *52*, 264.

(17) Okazaki, S.; Kuramochi, K. *Nippon Kagaku Kaishi* **1982**, 1141.

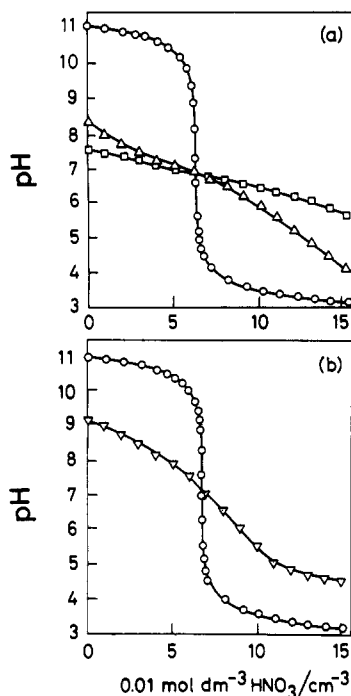
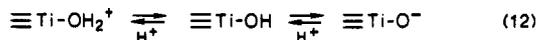


Figure 4. Potentiometric titration curves of (a) anatase and (b) rutile TiO₂ suspensions: O, without TiO₂; ▽, 1.0 g; Δ, 5.0 g; and □, 10.0 g of TiO₂.

curves intersected each other on a unique point around pH ≈ 7. The pH values of the intersecting points (pH_{ip}) are collected in Table I.

The amphoteric character of surface hydroxyl groups, schematically shown in eq 12,¹⁶⁻¹⁸ seems to account for the above-



mentioned results. Although several reports on the surface hydroxyl groups pointed out the existence of multiple sites with different acidity constants,^{16,19-21} we suppose the following formal equilibria among $\equiv\text{Ti}-\text{OH}_2^+$, $\equiv\text{Ti}-\text{OH}$, and $\equiv\text{Ti}-\text{O}^-$ to evaluate acidity constants, for convenience.

On assumption of these equilibria, the acidity constants of different forms of surface hydroxyls were estimated following the previous work by Schindler and Gamsjager.¹⁸ First, the difference between the amounts of the protonated ($\equiv\text{Ti}-\text{OH}_2^+$) and the deprotonated ($\equiv\text{Ti}-\text{O}^-$) hydroxyl groups (Γ^+ and Γ^- , respectively) was calculated from the difference in pH of the solution in the presence and absence of TiO₂, as follows:

$$\Gamma^- - \Gamma^+ = V[(C_H - C_{\text{OH}}) - (C_H - C_{\text{OH}})_{\text{init}}]/m \quad (13)$$

where V is the volume of the suspension, m is the weight of the TiO₂ powder, $(C_H - C_{\text{OH}})$ is the difference in the concentration between protons and hydroxide ions in the presence of TiO₂, and $(C_H - C_{\text{OH}})_{\text{init}}$ is the same difference in the absence of TiO₂. Figure 5 shows plots of $(\Gamma^- - \Gamma^+)$ as a function of pH of the suspension. The excess amount of hydroxyls ($\Gamma^- - \Gamma^+$) is independent of the amount of anatase TiO₂ suspended in the aqueous solution.

Since coexistence of $\equiv\text{Ti}-\text{OH}_2^+$ and $\equiv\text{Ti}-\text{O}^-$ is unlikely except for a narrow range around the intersecting point, the following simplifications may be permitted.

$$\text{if } C_H - C_{\text{OH}} > 0 \quad \text{then } \Gamma^- = 0 \quad (14)$$

$$\text{if } C_H - C_{\text{OH}} < 0 \quad \text{then } \Gamma^+ = 0 \quad (15)$$

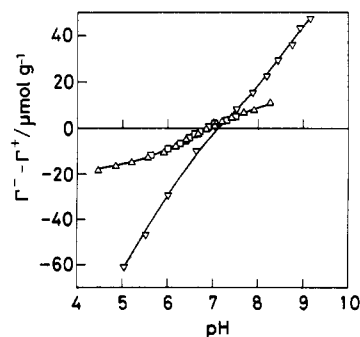


Figure 5. Excess amount of hydroxyls ($\Gamma^- - \Gamma^+$) on the surface of anatase (Δ , 5.0 g; \square , 10.0 g) and rutile TiO₂ (∇ , 1.0 g).

The data thus obtained were used to evaluate the amounts of hydroxyls in the protonated, neutral, and deprotonated forms, as shown in Figure 6. For this calculation the total amount of the surface hydroxyls (S), i.e., the sum of the protonated, neutral, and deprotonated hydroxyls, was estimated by extrapolation of $1/\Gamma^+$ (or $1/\Gamma^-$) vs. $1/C_H$ (or $1/C_{\text{OH}}$) plots (Table I). (The total amounts obtained from Γ^+ and Γ^- were practically identical in each TiO₂ system.) The total amount of surface hydroxyls on rutile TiO₂, $133 \mu\text{mol g}^{-1}$, was >6 times larger than that on anatase TiO₂.

On the basis of the results (14 OH nm^{-2} on anatase) by Boehm¹⁶ and the specific surface area, the amount of hydroxyl groups of $21.4 \mu\text{mol g}^{-1}$ corresponds to ca. 9% of the surface coverage of anatase TiO₂. It follows that >90% of the surface sites, i.e., oxygen atoms and/or ions, have not been detected under these experimental conditions. Boehm has also reported that only ca. 30% of hydroxyls on P-25 TiO₂ were detected by the titration with acids or bases.¹⁶ Since several reports on the surface hydroxyl groups pointed out the existence of multiple sites with different acidity constants, these underestimations of hydroxyls are attributable to the strongly acidic or basic hydroxyl group which could be detected under more acidic or basic conditions. The measurement of Ag⁺ adsorption on TiO₂ (as described in the following section) suggested the importance of such acidic sites. In the present study, we could evaluate the acidity constants for the detectable hydroxyl groups on the assumption of the equilibria represented as eq 12.

for the equilibrium: $\equiv\text{Ti}-\text{OH}_2^+ \rightleftharpoons \equiv\text{Ti}-\text{OH} + \text{H}^+$

$$K_{a1} = [\text{H}^+][\equiv\text{Ti}-\text{OH}]/[\equiv\text{Ti}-\text{OH}_2^+] = C_H(S - \Gamma^+)/\Gamma^+ \quad (16)$$

for the equilibrium: $\equiv\text{Ti}-\text{OH} \rightleftharpoons \equiv\text{Ti}-\text{O}^- + \text{H}^+$

$$K_{a2} = [\text{H}^+][\equiv\text{Ti}-\text{O}^-]/[\equiv\text{Ti}-\text{OH}] = C_H\Gamma^-/(S - \Gamma^-) \quad (17)$$

The calculated values were strongly dependent on the concentration of $\equiv\text{Ti}-\text{OH}_2^+$ and $\equiv\text{Ti}-\text{O}^-$, respectively. Assuming the linear relations between $\text{p}K_a$ and Γ , one can obtain

$$\text{p}K_{a1} = a + b\Gamma^+ \quad (18)$$

$$\text{p}K_{a2} = c + d\Gamma^- \quad (19)$$

These constants obtained from Figure 7 are listed in Table I.

Schindler and Gamsjager¹⁸ pointed out the effect of surface charge on the TiO₂ suspension. For proposing a quantitative interpretation, they assumed that (i) interactions between dispersed particles are negligible and (ii) the Gibbs energy of deprotonation is separable into ΔG_{int} (the energy of dissociation) and electrical work for the removal of the proton against the electrostatic field of the charged groups from the site of dissociation into the bulk of the solution

$$K_a = K_{a,\text{int}} \exp(F\Psi/RT) \quad (20)$$

where $K_{a,\text{int}}$ is the intrinsic acidity constant, i.e., the acidity constant

(18) Schindler, P. W.; Gamsjager, H. *Discuss. Faraday Soc.* **1971**, *52*, 286.

(19) Morterra, C.; Ghoti, G.; Garrone, E. *J. Chem. Soc., Faraday Trans. 1* **1980**, *76*, 2102.

(20) Brazdil, J. F.; Yeager, E. B. *J. Phys. Chem.* **1981**, *85*, 1005.

(21) Sham, T. K.; Lazarus, M. S. *Chem. Phys. Lett.* **1979**, *68*, 426.

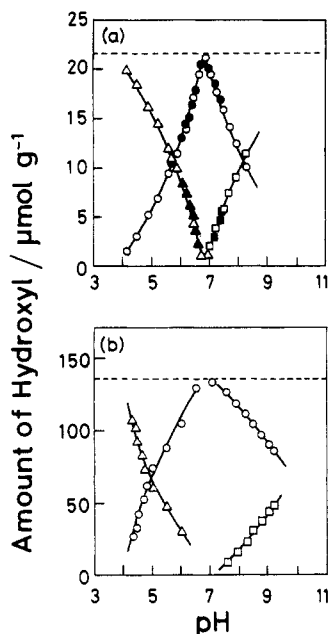


Figure 6. Distribution of protonated ($\equiv\text{Ti}-\text{OH}_2^+$, Δ and \blacktriangle), neutral ($\equiv\text{Ti}-\text{OH}$, \circ and \bullet), and deprotonated ($\equiv\text{Ti}-\text{O}^-$, \square and \blacksquare) hydroxyl groups on (a) anatase and (b) rutile TiO_2 surface. Broken lines represent the total amount of hydroxyls (S ; see Table I). Open symbols are data obtained by using (a) 5.0 g and (b) 1.0 g of TiO_2 . Closed symbols are data obtained by using (a) 10.0 g of TiO_2 .

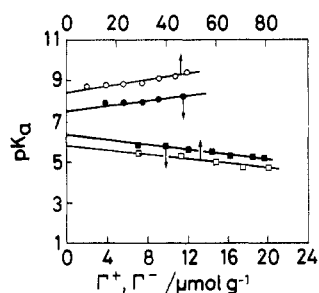


Figure 7. Dependence of pK_a on Γ^- and Γ^+ : (\bullet and \circ) Γ^- vs. pK_{a2} of anatase and rutile TiO_2 , respectively; (\blacksquare and \square) Γ^+ vs. pK_{a1} of anatase and rutile TiO_2 , respectively.

of the group in the absence of an electric field, and Ψ is the potential difference between the site of dissociation and the bulk of the solutions. The logarithm of eq 20 is formally consistent with eq 18 and 19. Therefore, intrinsic acidity constants (a and c) could be obtained (Table I).

Furthermore, the pH value of the system at which the amounts of $\equiv\text{Ti}-\text{O}^-$ and $\equiv\text{Ti}-\text{OH}_2^+$ are identical (pH_{EABP} : equi-acid-base point)²² can be estimated from eq 16 and 17, because participation of electrostatic field should be negligible around pH_{EABP} , as follows.

$$\text{pH}_{\text{EABP}} = (\text{p}K_{a1,\text{int}} + \text{p}K_{a2,\text{int}})/2 \quad (21)$$

In accord with the foregoing derivation, apparently good agreement between pH_{ip} and pH_{EABP} was obtained for both TiO_2 powders (Table I).

The reported values of a commercially available TiO_2 , P-25,¹⁸ are also listed in Table I. The total amount of surface hydroxyls of P-25 ($460 \mu\text{mol g}^{-1}$) and the surface area ($56 \text{ m}^2 \text{ g}^{-1}$) are significantly larger than those of TiO_2 used in the present investigation. The absolute values of the second terms of eq 18 and 19 (b and d , respectively) for anatase TiO_2 are extremely large

(22) Equi-acid-base point (EABP) is defined as an equiadsorption point (EAP) in the case that H^+ and OH^- are adsorbed on an oxide surface. On the other hand, the isoelectric point (IEP) is estimated by the measurement of dynamic characteristics of suspension, such as electrophoresis. EABP and IEP are often called the zero point of charge (zpc). They are essentially different in definition, though it is often the case that they are practically identical. In this paper, the term EABP was used in a strict manner.

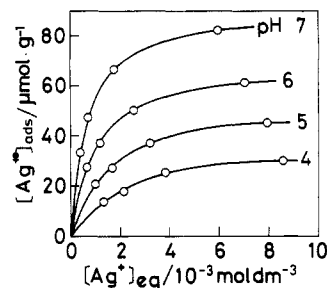


Figure 8. Amount of Ag^+ adsorbed onto the anatase TiO_2 surface ($[\text{Ag}^+]_{\text{ads}}$) as a function of equilibrium concentration of Ag^+ ($[\text{Ag}^+]_{\text{eq}}$) in the solution.

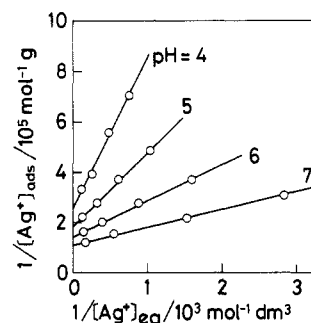


Figure 9. Reciprocal plots of $[\text{Ag}^+]_{\text{ads}}$ and $[\text{Ag}^+]_{\text{eq}}$ at various pH. Data were obtained from Figure 8.

TABLE II: Observed Constant for Ag^+ Adsorption on the Anatase TiO_2 Powder Suspended in AgNO_3 Solution and Amount of Hydroxyl Groups in the Neutral and Acidic Forms

pH	T^a , $\mu\text{mol g}^{-1}$	$10^{-3} K^b$	$\ln K$	$[\equiv\text{Ti}-\text{OH}]^c$, $\mu\text{mol g}^{-1}$	$[\equiv\text{Ti}-\text{OH}_2^+]^c$, $\mu\text{mol g}^{-1}$
7	89.5	1.67	7.42	21.3	≈ 0
6	68.8	1.06	6.97	13.0	8.3
5	55.0	0.62	6.43	6.0	15.3
4	38.9	0.44	6.08	1.1	20.2

^a Limiting amount of Ag^+ adsorption sites on the TiO_2 surface. ^b Equilibrium constant of Ag^+ adsorption. ^c Obtained from Figure 6.

compared to those for P-25 and rutile TiO_2 .

Correlation between Ag^+ Adsorption and pH-Dependent Chemical Structure of TiO_2 Surface. It is evident from Figures 2 and 6 that the positively charged surface inhibits the Ag^+ adsorption; pH dependences of Ag^+ adsorption and surface hydroxyl deprotonation were quite similar. Electrostatic repulsion between positive surface charge, due to the protonation of surface hydroxyls, and Ag^+ accounts for this phenomenon. Figure 8 shows the amount of adsorbed Ag^+ ($[\text{Ag}^+]_{\text{ads}}$) on the anatase TiO_2 surface as a function of the equilibrium concentration of Ag^+ ($[\text{Ag}^+]_{\text{eq}}$) at a given pH (data are derived from Figure 2). It is clear that $[\text{Ag}^+]_{\text{ads}}$ becomes a plateau over the $[\text{Ag}^+]_{\text{eq}}$ range of $>5 \text{ mmol dm}^{-3}$; the saturation limit increases with the increasing pH from 4 to 7 (see also Figure 2). Double reciprocal plots were practically linear at each pH (Figure 9), showing that the absorptions fit a formal Langmuir equation

$$[\text{Ag}^+]_{\text{ads}} = TK[\text{Ag}^+]_{\text{eq}} / (1 + K[\text{Ag}^+]_{\text{eq}}) \quad (22)$$

where T and K represent the limiting amount of adsorption site and adsorption equilibrium constant, respectively. Both values of T and K decreased as pH decreased, and thus the positive charge on the TiO_2 surface increased (see Table II). The fact that there were at least 5 times more sites for Ag^+ than for H^+ at pH 7 suggests that the surface sites for such Ag^+ adsorption are predominantly ascribed to the strongly acidic hydroxyls, which are not detected by the present titration method.

Rutile TiO_2 has almost equal or slightly larger specific surface area (Table I) compared with anatase TiO_2 . However, $[\text{Ag}^+]_{\text{ads}}$ was significantly smaller than anatase TiO_2 . This is attributable to the smaller amount of the strongly acidic hydroxyls on rutile

TiO₂, because of the >6 times greater amount of the weakly acidic surface hydroxyls.

Conclusion

The significant pH dependence of the photocatalytic activity of TiO₂ suspended in AgNO₃ solution was correlated with the pH-dependent adsorption of Ag⁺ on the TiO₂ surface. The adsorbed Ag⁺ seemed to exhibit the efficient ability to trapping photogenerated electrons, thereby enhancing the oxidation of water by the simultaneously generated positive holes. From the results of quantitative analysis of surface hydroxyls, the pH dependence of Ag⁺ adsorption was attributed to the positive surface charge on TiO₂. Consequently, a TiO₂ powder having a large surface area with a high proportion of strongly acidic surface sites rather

than readily protonated hydroxyls is favorable for the photocatalytic reaction.²³ The rutile TiO₂ used in this study was disadvantageous due to the extensively higher surface density of the readily protonated hydroxyls. The effect of surface treatments on the improvement of photocatalytic activity is now under investigation.

Registry No. TiO₂, 13463-67-7; AgNO₃, 7761-88-8; H₂O, 7732-18-5; Ag, 7440-22-4; O₂, 7782-44-7.

(23) A similar conclusion was derived by Oosawa and Grätzel. They reported that the photocatalytic activity of TiO₂ suspended in an AgNO₃ solution was proportional to the reciprocal of the surface hydroxyl density: Oosawa, Y.; Grätzel, M. *J. Chem. Soc., Chem. Commun.* 1984, 1629.

Analysis of Paired Interacting Orbitals for Extended Systems. Application to the Protonation of Conjugated Carbon Chains and the Chemisorption of H₂ on Ni Surfaces

Hiroshi Fujimoto* and Hiroshi Kawamura

Division of Molecular Engineering, Kyoto University, Kyoto 606, Japan (Received: September 23, 1986)

The protonation of conjugated carbon chains and chemical interactions between H₂ and nickel layers have been investigated theoretically. The analysis is based on the paired interacting orbitals which conveniently illustrate interactions between two systems. The interacting orbitals of clusters are compared with those of an extended sequence of cells with respect to protonation of conjugated carbon chains. Then, the orbitals are shown to vary in chemisorption on metal surfaces, reflecting the mode of the interaction. It is shown that electron delocalization takes place on the face but that the overlap repulsion penetrates into the inner layers. The effects of cluster size on these bonding and antibonding interactions are discussed.

Introduction

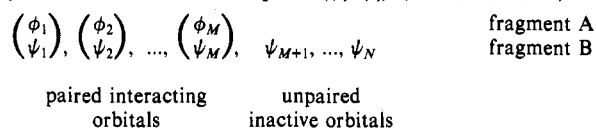
The concept of orbital interaction is a powerful strategy in chemistry.^{1,2} A number of experiments have been rationalized in terms of the frontier orbital interactions. On the other hand, we have shown in our previous papers that the local characteristics of chemical interactions can be displayed more properly by some sort of localized orbitals.³ They have been derived as the hybrids of usual molecular orbitals (MO's) by means of a pair of transformations of fragment orbitals for each given interaction.⁴ This theoretical treatment will be of great use when we discuss chemical interactions of large systems, e.g., reactivities and catalytic activities of organometallic systems and solid surfaces. In this paper, we study adsorption of small chemical species to conjugated carbon chains and onto nickel films. We present the orbitals that participate actively in chemical interactions in these systems.

Method

Let us consider an interaction between two molecular systems A and B. In the following discussion, A is assumed to be a small species and B is either a cluster of atoms or a unit cell of a polymeric molecule. The electronic structure of the composite interacting system A-B can be determined by using the usual MO methods or the tight-binding calculations.⁵ The interaction is represented in terms of various quantities associated with the first-order density matrix **P**, the (*r*, *s*) element of which is defined for the atomic orbital (AO) χ_r (*r* = 1, 2, ..., *M*) of A and the AO

χ_s (*s* = *M* + 1, *M* + 2, ..., *M* + *N*) of B. The intermolecular part of this matrix is rectangular and in general of the order *M* × *N*. (*M* is assumed to be smaller than *N*.)

By carrying out the coupled transformations of AO's or MO's within each of the two fragments simultaneously, one can reduce intermolecular part of this matrix to the form that has nonzero elements solely between several sets of paired interacting orbitals of the two fragments.⁴ Now, the interaction is described simply by means of these orbital pairs (ϕ_i, ψ_i) (*i* = 1, 2, ..., *M*).



The number of orbital pairs is determined by the smaller entity. For instance, H⁺ has a single orbital in minimal basis set calculations and, accordingly, the intermolecular part of the bond order matrix will have a single nonzero element upon transformation, i.e., *M* = 1 and, therefore, $P'_{i,i} = 0$ for *i* ≠ 1. The interaction is represented simply by the 1s AO of the proton and one of the new rehybridized MO's of the larger fragment, irrespective of its size. As a consequence, a direct comparison of chemical interactions is attainable for systems analogous in character but different in molecular size.

Results and Discussion

A Comparison of Crystal and Cluster Interacting Orbitals. Let us examine first of all the simplest system, an interaction between a proton and a conjugated carbon chain as sketched in Figure 1. A unit cell of the polymer chain was taken tentatively to be C₂H₂, C₆H₆, and C₁₀H₁₀, and the electronic structures of the composite interacting system, e.g., (-CH=CH- + H⁺)_n, were determined by tight-binding calculations of the extended Hückel type.⁵ A proton was located tentatively at 1.5 Å above the midpoint of the central C-C double bond in each case. Here the transformations of orbitals were carried out between a proton and the carbon chain.

(1) Fukui, K. *Theory of Orientation and Stereoselection*; Springer-Verlag: West Berlin, 1974.

(2) Hoffmann, R. *Angew. Chem., Int. Ed. Engl.* 1982, 21, 711.

(3) Fujimoto, H.; Koga, N.; Fukui, K. *J. Am. Chem. Soc.* 1981, 103, 7452.

(4) (a) Fujimoto, H.; Koga, N.; Hataue, I. *J. Phys. Chem.* 1984, 88, 3539. (b) Fujimoto, H.; Yamasaki, T.; Mizutani, H.; Koga, N. *J. Am. Chem. Soc.* 1985, 107, 6157. (c) Fujimoto, H.; Yamasaki, T. *Ibid.* 1986, 108, 578.

(5) (a) Bloch, F. *Z. Phys.* 1928, 52, 555. (b) Imamura, A. *J. Chem. Phys.* 1970, 52, 3168. (c) Hoffmann, R. *J. Chem. Phys.* 1963, 39, 1397. (d) IMS Computer Center Library Program No. 1103.